Arabian Journal of Chemistry (2021) **14**, 103021

King Saud University

Arabian Journal of Chemistry

www.ksu.edu.sa
www.sciencedirect.com

ORIGINAL ARTICLE

In-vitro and *in-silico* antioxidant, α-glucosidase inhibitory potentials of abutilins C and D, new flavonoide glycosides from *Abutilon pakistanicum*

Muhammad Imran [a,b,*], Ahmad Irfan [a,c,*], Muhammad Khalid [d], Noreen Khalid [e], Jalal Uddin [f], Riaz Hussain [g], Bakhat Ali [d], Mohamed Hussien [a,h], Mohammed A. Assiri [a], Abdullah G. Al-Sehemi [a]

[a] *Department of Chemistry, Faculty of Science, King Khalid University, P.O. Box 9004, Abha 61413, Saudi Arabia*
[b] *Department of Chemistry, Ghazi University Dera Ghazi Khan, Pakistan*
[c] *Research Center for Advanced Materials Science (RCAMS), King Khalid University, P.O. Box 9004, Abha 61413, Saudi Arabia*
[d] *Department of Chemistry, Khawaja Fareed University of Engineering and Information Technology, Raheem Yar Khan, Pakistan*
[e] *Faculty of Pharmacy, University of Sargodha, Punjab, Pakistan*
[f] *Department of Pharmaceutical Chemistry, College of Pharmacy, King Khalid University, P.O. Box 9004, Abha 62529, Saudi Arabia*
[g] *Department of Chemistry, Division of Science & Technology, University of Education, Township, Lahore, Pakistan*
[h] *Pesticide Formulation Department, Central Agricultural Pesticide Laboratory, Agricultural Research Center, Dokki, Giza 12618, Egypt*

Received 24 October 2020; accepted 11 January 2021
Available online 28 January 2021

KEYWORDS

Abutilon pakistanicum;
Abutilin C-D;
Antioxidant activity;
α-glucosidase inhibition;
Quantum chemical study;
Molecular docking

Abstract The methanolic extract along its various fractions *Abutilon pakistanicum* were analyzed to find total phenolic, flavonoids contents followed by antioxidant and α-glucosidase inhibitions of isolated pure constituents. The total content of phenolics and flavonoids was consistently higher in CH_2Cl_2 (54.89 and 56.06 mg/g extract respectively) compared with *n*-hexane, ethyl acetate, *n*-butanol and H_2O portions (ranging between 37.81–54.89 and 38.11–56.06 mg/g extract). In order to determine active biological ingredients from CH_2Cl_2 subportions, extensive advanced chrotapographic separation methods resulted isolation of new flavonoid glycosides namely abutilins C-D (**1**–**2**). The structures of these constituents were interpreted by spectroscopic data including FAB-MS, ESI-MS, 1D and 2D-NMR experiments. Both flavonoid (**1**–**2**) were evaluated against antioxidant and α-glucosidase inhibitory assay. The antioxidant potential of dichloromethane extract and abutilins C-D (**1**–**2**) were determined using DPPH and nitric oxide radial scavenging assays. The abu-

* Corresponding authors at: Department of Chemistry, Faculty of Science, King Khalid University, P.O. Box 9004, Abha 61413, Saudi Arabia.
E-mail addresses: imranchemist@gmail.com (M. Imran), irfaahmad@gmail.com (A. Irfan).
Peer review under responsibility of King Saud University.

Production and hosting by Elsevier

https://doi.org/10.1016/j.arabjc.2021.103021

tilins C displayed significant inhibition, with IC_{50} values 41.66 (DPPH), 39.04 (NOS) μg/mL, using positive control ascorbic acid and quercetin respectively. Inhibitory effects of flavonoids against enzyme α-glucosidase were also investigated and abutilins C showed significant activity with IC_{50} values 8.27 μg/mL compared with positive control ascarbose (IC_{50}, 5.92 μg/mL). Abutilins C can serve dual inhibitors as antioxidant agent and to treat α-glucosidase associated diseases. Phytochemicals geometries i.e ground state were optimized by density functional theory (DFT) B3LYP/TZ2P to understand the electronic properties of the studied compounds. The ground state geometries of abutilin_C, abutilin_D and reference compounds were optimized by DFT then various electronic properties were explored. Moreover, we have also investigated the global molecular descriptors, molecular electrostatic potential, Hirshfeld analysis and molecular docking by quantum chemical calculations.

1. Introduction

Primitive source of about 25% modern medications are plants, which have been used as therapeutic agents against various diseases for more than 5000 years. *Abutilon* belongs to family Malvaceae, wide spread in sub-tropical and tropical regions around world as a small trees, shrubs and perennial herbs, used as demulcents, diuretics and for treatment of rheumatism (Ali et al., 2014, 2010). *Abutilon pakistanicum is* a member of the genus *Abutilon* native to Pakistan. The reported constituents from *A. pakistanicum* are phenolic acids *p*-coumaric, vanillic, *p*-hydroxybenzoic, and caffeic, Abultin A-B, Ferulic acid, 5-hydroxy-4,6,7,8-tetramethoxyflavone, (*E*)- cinnamic acid, kaempferol, luteolin and luteolin glucopyranoside (Ali et al., 2010). Another study on *A. pakistanicum* reported the presence of pakistoside A-B, kaempferol, kaempferol-3-rhamnopyranoside and luteolin.

Polyphenols like flavonoids, water-soluble antioxidants are thought to be beneficial for human beings as their free radicals scavenger ability along with reactive oxygen species (ROS) capability (Meng et al., 2019). The antioxidant active constituents are widely present in a large number of aromatic and other medicinal plants. The atomic orbital containig electron (unpaired) termed free radicals like ROS exist independently. These ROS initiate the chain reaction, propogate resulting cell reptures. The antioxidants controlled the concentration of ROS substances within cell via free radical scavenging, lipid peroxidation prevention along with catalytic metal ions chelation (Valko et al., 2016). Human health in medicine field is significantly affected by natural phytochemicals, like antioxidants (radical scavengers or antiradical). Furthermore, phytochemicals helps to protect human beings from oxidative impair, securing cells from radicals and hamper from acute diseases (Saffarzadeh-Matin and Khosrowshahi, 2017). These natural antioxidants considered harmless as compared with synthetic compounds (Nasri et al., 2015).

Diabetes considered as major health issue having 629 million people (90–95%) suffering from disease i.e diabetes. It is conssidered as important task for the scientists working in nutrition, food and medical science fields. Polyphenols and flavonoids beneficial effects are well known and have become an area of great consern in recent years. For insulin independent diabetes, polyphenols have been found to inhibit glucose absorption within gastrointestinal tract, digestive enzymes inhibition specified for carbohydrate breakdown and modification of energy metabolism/energy status. Recently, it has also been shown that phenolics/flavonoids play potential role to cure diabetes (Sadeer et al., 2019). Acarbose is a medicine clinically used to inhibit digestive enzymes ability such as α-glucosidase and α-amylase. Unfortunately, its long-term administration resulted by side-effects including diarrhea and abdominal distention. Based on safety potential alternative natural products may also be used to cure diabetes. The antioxidant and α-glucosidase inhibition of flavonoids have not yet been explored and few literature is available about the flavonoids (Zhu et al., 2019). Therefore, the ethnopharmacological and chemotaxonomic importance of *A. pakistanicum* has provoked us for further phytochemical investigation. In present work total phenolic contents (TPC) and total flavonoid contents (TFC), analysis of polyphenolic compounds were determined from crude extracts and its fractions. Based on initital screening the dichloromethane fractions of *A. pakistanicum* resulted isolation of pure constituents having antioxidant (DPPH and NO scavening) and α-glucosidase inhibition potential.

The density functional descriptors regarding quantitative structure–activity relationship (QSAR), consedered as essential in order to determine interaction nature, active sites and phytochemicals biological potential. To explore the interesting biological and pharmacological activities, its noteworthy to shed light on various molecular descriptors, frontier molecular orbitals-FMO, ionization potential-IP, electron affinity-EA, molecular electrostatic potential-MEP, and Hirshfeld analysis. These computations employed to understand the active sites which have been investigated in current research work and discussed with detail. We have also shed light on the global reactivity descriptors-GRD, *e.g.,* electronegativity-χ, chemical potential-μ, chemical hardness-η, electrophilicity index-ω and softness-S.

To conclude the objectives of current research work to: (i) bioguided fractionation of methanolic extract of *A. pakistanicum*; (i) bioguided isolation from CH_2Cl_2 fraction resulted flavonoids (see Fig. 1); (iii) investigate their antioxidant (DPPH and NO scavenging assay) and α-glucosidase activity; (iv) exploration of electronic properties, structure–activity relationship and molecular docking. The results attained may used provided guidance to design drugs as antioxidant and to cure diabetic patients.

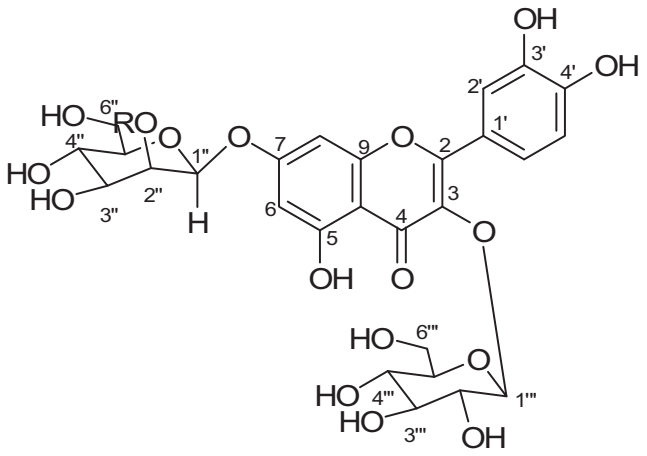

Fig. 1 Structures of abutilins C (**1**) and D (**2**).

2. Materials and methods

2.1. General

The column chromatography (CC) was carried out using silica gel (230–400 mesh, E. Merck, Darmstadt/Germany). For UV/IR spectra with UV-3200 (Hitachi)/302-A Jasco) spectrophotometer were used. EI-MS, FAB-MS performed on a MAT 312 MS (Finnigan) and JMS-HX-110 MS (JEOL) with glycerol as a matrix respectively. The AMX-500 spectrometer (Bruker) to get the ^{1}H–^{13}C NMR spectra with solvent C5D5N contains tetramethylsilane (TMS) as internal standard. The 2D NMR (COSY, HMQC, HMBC, NOESY) spectra were recorded within same instrument. Thin layer chromatography (TLC) accomplished with silica gel (F_{254}, E. Merck, Germany) precoated plates and spots were visualized with UV light (254 and 366 nm). Reference compounds of flavonol glycosides and biological activity standards were purchased from Sigma-Aldrich, Germany.

2.2. Plant material

The *Abutilon pakistanicum* (Malvaceae), whole specimen was collected at Karachi, Pakistan in June 2016. Department of Botany UOK plant taxonomist Prof. S Khatoon identified the plant material as a taxonomist, where 697 KUH voucher number deposited in the herbarium.

2.3. Extraction and isolation

Powder of air-dried *A. pakistanicum* (8 kg) was soaked in MeOH thrice to get the extract, which was concentrated in vacuo to get blackish crude extract. This semi-solid crude was suspended in H_2O and by using solvent–solvent extraction procedure this was divided into different polarity organic solvents and water-soluble fractions. CH_2Cl_2 sub-portion was subjected to CC over silica gel eluting with organic solvents in increasing order of polarity. Currently, CH_2Cl_2 portion was subjected to silica gel CC and eluted with organic solvents with increasing polarity, which yielded six major sub-fractions (Fr. 1 to Fr. 6). Fraction 5 and 6 showing the presence of flavonoidal glycoside within TLC. Repeated CC by fraction 5 yielded new abutilin A and B reported in our paper previously (Ali et al., 2010). The fraction 6 was eluted with CH_2Cl_2-MeOH with increasing polarity to yield four sub-fractions (Fr. A to Fr. D). Fraction C was subjected to final purification with CC using silica gel (230–400 mesh size) as adsorbent with mobile phase DCM-MeOH (90:10) to yield abutilin C (12 mg) and fraction D (0.31 g) was subjected to CC with DCM-MeOH (85:15) to yield abutilin D (10 mg).

2.4. Total phenolic and flavonoid contents

The method used to determine the TPC employed by Folin-Ciocalteu colorimetric method. Briefly, for TPC extracts each prepared sample was incubated and absorbance at UV–Vis. spectrophotometer (760 nm) was recorded. This was calibrating against the standards as gallic acid and attained values were expressed as (mg) gallic acid equivalent per (g) extract i.e (mg of GAE/g) (Vats, 2016).

Alike, total flavonoid contents (TFC) have been calculated following previously standard calorimetric methods (Cenobio-Galindo et al., 2019). After incubation of each sample, its absorbance value was determined at 415 nm. The amount of total flavonoids-TFC were uttered as rutine quivalents (mg RE/g extract). For both TPC/TFC calculation, triplicate experiments readings were determined, and results were averaged.

2.5. Characterizations of abutilins C (*1*)

Yellow gum. UV (MeOH): 262 (3.1), 274 (2.7), 354 (2.5). IR (KBr): 3350–3745 (br. s), 1654, 1550, 1505, 1297, 1064, 630. ^{1}H- ^{13}C NMR: see Table 2. FAB-MS (pos.):627 ($[M+H]^+$), 463 ($[M-H-hex]^+$), 300 ($[M-2H-2hex]^+$). EI-MS: 301 (30), 300 (10), 285 (17), 160 (15), 151 (30), 150 (32), 125(10), 110 (35). HR-FAB-MS (pos.): 627.1472 ($[M+H]^+$, $C_{27}H_{31}O_{17}$; calc. 627.1483).

2.6. Characterizations of abutilins D (*2*)

Yellow gum. UV (MeOH): 264 (3.0), 273 (2.8), 355 (2.5). IR (KBr): 3355–3730 (br. s), 1660, 1545, 1510, 1295, 1060, 637. ^{1}H- ^{13}C NMR: see Table 2. FAB-MS (pos.): 707.1037 ($[M+H]^+$), 544 ($[M+H\text{-hex}]^+$), 464 ($[M+H\text{-}SO_3hex]^+$), 302 ($[M+2H\text{-hex-}\ SO_3hex]^+$). EI-MS: 300 (10), 285 (17), 160 (15), 151 (30), 150 (32), 125(10), 110 (35), 97 (20), 80 (15). HR-FAB-MS (pos.): 707.1037 ($[M+H]^+$, $C_{27}H_{31}O_{20}S$; calc. 707.1051).

2.7. Antioxidant bioassay

Antioxidant bioassay was done by DPPH and NO scavenging assay based on the principle that a -H donor is an antioxidant. The potential of antioxidant is proportional to DPPH and NO radical disappearance within sample. The test sample was prepared according to standard procedure (Sharma and Cannoo,

2017) and absorbance of the each sample was determined at 518 nm by using ascorbic acid and quercetin as reference standards (positive controls). The % age DPPH scavenging activities of the dichloromethane extracts, abulitin C-D and ascorbic acid was calculated by using equation:

$$\text{Inhibition}(\%) = 100 - (\text{Absorbance of test sampleAbsorbance of control}) \times 100.$$

2.8. α- glucosidase inhibition assay

It was measured by the standard method with slight modifications (Tanase et al., 2019). Enzyme α-glucosidase solution (0.2 U/ml), sample solution (60 µl) phosphate buffer 0.1 M having pH 6.9 (50 µl) incubated in 96 well plates for 10 min at 40 °C. The 50 µl of 5 mM *p*-nitrophenyl-α-D-glucopyranoside in pesence of same buffer solution added to each well and incubated for minute (10) at 40 °C. It was quenched by adding 0.2 M $NaCO_3$ (150 µl) within well that were analyzed, and its absorbance were recorded at 405 nm using ascarbose (+ive control). The % age enzyme inhibition was determined by using equation:

$$Inhibition(\%) = 100 - (Abs\ of\ test\ sampleAbs\ of\ control \times 100)$$

EZ-Fit Enzyme Kinetics Software used for calculation of IC_{50} values (concentration at which 50% enzyme catalyzed reaction occurs) of phytochemicals.

2.8.1. Optimization of assay conditions

Optimization of reaction conditions were done by OVAT (one variable at a time) technique. Different chemical parameters were investigated including buffers, solvents, enzyme concentration and substrate concentration. Concentration of α-glucosidase enzyme were studied in the range of 0.0–0.12 units/well keeping the substrate concentration constant at 10 µl/well of 0.5 mM. Enzyme concentration of 0.057 unit/well was found optimum for α-glucosidase owing to maximum response and strength of reading (as shown in Fig. 2). Keeping the enzyme concentrations constant, different concentrations of substrate (ρ-nitrophenyl-α-D-glucopyranoside) were investigated in the range of 0–20 µl/well of 0.5 mM of substrate. Out of these substrate concentrations 10 µl/well was found optimum α- glucosidase for studies and it was finalized for further studies (Fig). All the finalized parameters discussed above were used for temperature studies done in the range of 10–40 °C. Among these 30 °C was found the most suitable for α-glucosidase in our laboratory conditions.

2.9. Computational details

In order to probe the diverse properties of interests first-principles approach is an interesting tools (Anastassova et al., 2018; Irfan et al., 2019a, 2019b, 2019c; Rammohan et al., 2020; Wazzan and Irfan, 2019). The prediction of extensive electronic characteristics which may replicated the experimental results was measured with Density functional theory (DFT) (Irfan, 2019). Its authentic stategies for the measurement of different compounds ground state (S_0) geometries, optimization along with its electronic characteristics (Irfan et al., 2018; Irfan et al., 2020a, 2020b, 2020c). The B3LYP is sensible for the S_0 geometries of several phytochemicals (Preat et al., 2010). Shifting of literature revealed that after optimizing the geometries of phytochemicals with functional (B3LYP) with broad range of basis sets has no extraordinary effect on various geometrical parameters (Preat et al., 2009). Currently, optimizations were conducted by B3LYP functional with basis set as triple zeta with polarization function (TZP) (Irfan et al., 2013). The detailed computations were executed with ADF. Additionaly, for docking purposes Autodock version 4.2 was employed with H_2O molecule elimination succeeded by adding polar hydrogen. Autodock 4.2 endorsed using Autodock tools, MGL tools. To find location of binding site among native ligand Autogrid utilized with organizing the grid X, Y, and Z-axis coordinates. The Autodock 4.2 along with Pymol version 1.7.4.5 Edu softare employed for docking computations.

3. Results and discussion

3.1. Total phenolic content TPC and TFC

Total phenolic and flavonoid contents of crude methanol and its soluble organic fractions like hexane, CH_2Cl_2, EtOAc, *n*-butanol and H_2O extracts of *A. pakistanicum* presented in Table 1. According to our results, phenolic content of hexane, CH_2Cl_2, EtOAc, *n*-butanol and H_2O extracts were 45.15, 77.51, 54.89, 37.81 and 46.03 respectively. The TPC of *Abutilon pakistanicum* was evaluated Folin-Ciocalteu assay using standard gallic acid (GA) by plotting the relationship between absorbance vs concentration. The TPC of *Abutilon pakistanicum* result revealed that the phenolic compounds were best extracted dichloromethane for extraction having more amount of interesting phytometabolites.

Total flavonoids content was measured using a standard procedure (Genovese et al., 2020) using Rutin as positive control (standard). The TFC of the analyzed samples (Table 1) were expressed as mg rutine/g each extract. Each result represented the mean ± S.D. of three experimental determinations. According to our flavonoid contents results hexane, CH_2Cl_2, EtOAc, *n*-butanol and H_2O extracts were 44.91, 71.47, 56.06, 38.11 and 40.18 respectively, revealed the presence of high flavonoids within dichloromethane extract.

3.2. Abutilin C (*1*)

Bioguided directed isolation of dichloromethane soluble portions of *A. pakistanicum* using repeated column chromatography affoarded four new flavonoids namely Abutilin A-D. The spectral information of Abutilin A-B was reported by our previous study (Ali et al., 2010) and herin structural elucidation and antioxidants and α-glucosidase activity of Abutilin C-D was explained. Abutilin C (**1**) was obtained as a yellow gum from dichloromethane soluble fractions. The HRFABMS (+ive mode) of **1** showed a quasi-molecular-ion $[M+H]^+$ peak at *m/z* 627.1472, consistent with the M.F. $C_{27}H_{31}O_{17}$. The prominent peak in EI-MS exhibited at *m/z* 300 ($[M - 2 \times sugar]^+$), which indicate the loss of hexose moieties. The UV spectrum was characteristic of a flavonol, which exhibited maximum absorption at 262, 274 and 354 nm. The 40 nm bathochromic shift was seen with addition of $AlCl_3$/

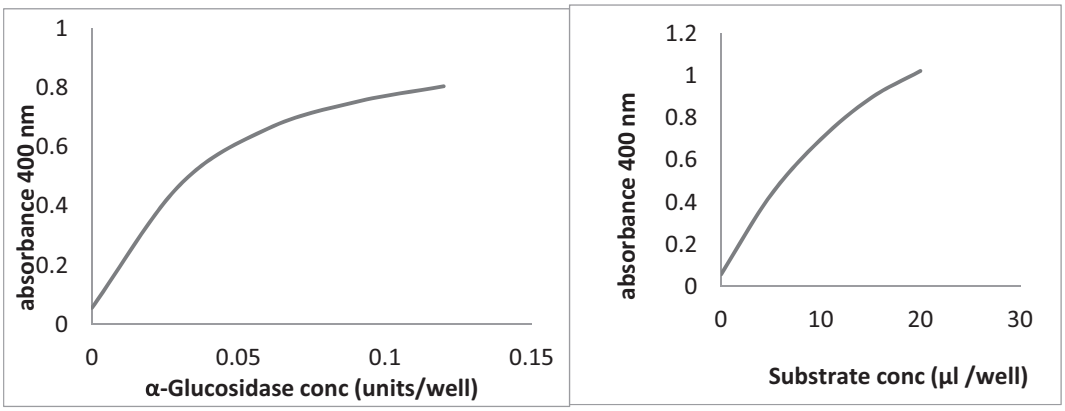

Fig. 2 a. Dose dependent curve of α-glucosidase b. Standard curve of substrate for α-glucosidase.

Table 1 Total phenol and flavonoid content of *Abutilon pakistanicum* extracts.

Plant extracts	Total phenol content (mg GAE/g extract)	Total flavonoid content (mg RE/g extract
n-hexane	45.15 ± 1.01	44.91 ± 0.94
CH_2Cl_2	77.51 ± 0.35	71.47 ± 1.03
ethyl acetate	54.89 ± 0.97	56.06 ± 1.11
n-butanol	37.81 ± 1.03	38.11 ± 0.58
water	46.03 ± 1.01	40.18 ± 0.87

GAE: Gallic acid equivalents; RE: Rutin equivalents. Data are expressed as mean ± SD.

Table 2 ^{1}H- ^{13}C NMR results of abutilin C (**1**) in C_5D_5N; δ in ppm, *J* in Hz.

No	Abutilin C (1)		
	δ_H	δ_C	HMBC
1	–	–	–
2	–	157.2	–
3	–	134.1	–
4	–	178.7	–
5	–	162.4	–
6	6.20 (d, *J* = 2.0)	99.2	5, 7, 10, 1″
7	–	162.9	–
8	6.37 (d, *J* = 2.0)	93.7	7,9,10
9	–	157.5	–
10	–	105.2	–
5-OH	13.5	–	–
1′	–	121.9	–
2′	7.42 (d, *J* = 2.1)	115.7	2, 1′, 3′, 4′
3′	–	145.3	–
4′	–	148.8	–
5′	6.85 (d, *J* = 8.4)	116.2	1′, 3′, 4′, 6′
6′	7.60 (dd, *J* = 2.1, 8.4)	121.8	2, 1′, 2′, 5′
1″	4.80 (d, *J* = 5.2)	107.2	7, 2″, 3″
2″	3.95–3.98 (m)	76.3	1″, 3″, 4″
3″	4.10–4.15 (m)	79.4	–
4″	4.18–4.20 (m)	72.7	–
5″	3.91–3.93 (m)	80.2	–
6″	4.46–4.48 (m)	62.9	–
	4.36–4.39 (m)		
1‴	5.30 (d, *J* = 7.5)	100.9	3, 2‴
2‴	4.28–4.31 (m)	73.9	–
3‴	4.21–4.24 (m)	76.4	–
4‴	4.34–4.38 (m)	70.9	–
5‴	4.40–4.43 (m)	77.8	–
6‴	4.50–4.53 (m)	62.5	–
	4.25–4.27 (m)		

HCl, revealed chelated —OH presence at C-5 of a flavonoid (Ali et al., 2010). The IR absorption band were evident of a —OH (3350–3745 cm^{-1}), carbonyl conjugated (1654 cm^{-1}) and aromatic moieties (1550 and 1505 cm^{-1}) and ether groups (1297, 1064, 630 cm^{-1}). The UV spectrum, IR peaks, ^{1}H NMR spectrum in pyridine d_5 indicated that **1** was a quercetin derivative. The ^{13}C NMR spectra exhibited 27 carbon signals corresponding to two methylene, fifteen methin and ten quaternary C-atoms (Table 2). The resonances of ring B were characteristic ABX spin system having resonances at δ_H 6.85 (H-5′, *d*, *J* = 8.4), 7.42 (H-2′, *d*, *J* = 2.1) and 7.60 (H-6′, *dd*, *J* = 2.1, 8.4). The two *meta*-coupled doublets in the ^{1}HNMR spectrum were exhibited at δ_H 6.20 (*d*, *J* = 2.0) and 6.37 (*d*, *J* = 2.0) corresponded to H-6 and H-8, were regarded to quercetin moiety. Instead of quercetin signals, the two sugar residues were revealed by the corresponding anomeric protons signals having doublets at δ_H 4.80 (*d*, *J* = 5.2) and 5.30 (*d*, *J* = 7.5).

The hexose units have larger coupling constant values endorsed for *β*-configuration assignment for hexoses moieties (Ali et al., 2012). Further signals of oxymethines were observed between δ_H 4.21–4.43 and 3.91–4.20 and oxymethylene at δ_H 4.25–4.27, 4.36–4.39, 4.46–4.48 and 4.50–4.53 for the sugar moities. The ^{13}CNMR signals at δ_C 157.2, 134.1, 178.7, 157.5 and 105.2 were typical of a flavonol moiety. The signals of benzene ring moiety were resonated at δ_C 115.7, 116.2, 121.8, 121.9, 145.3 and 148.8 forming an ABX system. The anomeric carbons were observed at δ 107.2 and 100.9 along with further signals of the hexose moieties. The ^{1}H -^{13}C NMR signal revealed towards skeleton as flavonoid class of quercetin type (Halabalaki et al., 2011). The acid hydrolysis of abutilin C provided quercetin and glycones binary mixture identified as D -glucose and D-mannose by TLC with standard

as well as by gas chromatography (GC) by comprising of retention times of their tetramethylsilane (TMS) ethers with corresponding standards (Miyazawa and Hisama, 2003). The 2D-HMBC experiments, position of D-glucose moiety was established in which the anomeric proton at δ_H 5.30 exhibited ^3J correlation with C-3 at δ_C 134.1 and also anomeric proton of D-mannose at δ_H 4.80 showed ^3J correlation with C-7 at δ_C 162.9. Thus above evidences support to allocate the D-glucose moiety at C-3 followed by D-mannose at C-7. Further, the HMBC correlations illustrated in Table 2 are in complete support with the assigned structure of abutilin C as quercetin-3-O-[β-D-glucopyranosyl]-7-O-β-D-mannopyranoside (Fig. 1).

3.3. Abutilin D (2)

It was obtained as a gummy yellow material from dichloromethane soluble extract which shows similar characteristics and tests as those of **1**. The HR-FAB-MS (positive mode) of abutilin D **2** gives a quasi-molecular-ion $[M+H]^+$ peak at m/z 707.1037, consistent with the molecular formula $C_{27}H_{31}O_{20}S$. The EI-MS exhibited prominent peak at m/z 300 ([M - hexose - SO_3hexose]$^+$), which indicate the loss of hexose moieties. The further ions fragment observed at m/z 97 and 80, confirmed the presence of sulfohexose moiety. Also the UV/IR spectra were alike to those of **1**. The ^{13}C NMR spectra (BB and DEPT) showed twenty-seven well-resolved carbon peaks corresponding to two CH_2, fifteen CH groups, and ten quaternary C-atoms (Table 3). Similar to compound **1**, meta-coupled doublets of H-6, 8 were resonated at δ_H 6.24 and 6.45 (J = 2.3 Hz). The resonances of ring B were characteristic ABX spin system having resonances at δ_H 6.84 (*d*, J = 8.5, H-5′), 7.43 (*d*, J = 2.5, H-2′) and 7.70 (*dd*, J = 2.5, 8.5, H-6′). The anomeric protons shows doublets at δ_H 4.85 (*d*, J = 5.0) and 5.32 (*d*, J = 7.5) in the spectrum. These coupling constant value larger, allowed β-configuration for both hexose units. The sugar moieties further showed signals for oxymethines between δ_H 4.20–4.43 and 3.83–4.54 and oxymethylene at δ_H 4.23 (dd, J = 5.1, 5.2), 4.27–4.29, 4.44–4.47 and 4.50–4.54. Further the double doublet appeared at δ_H 5.10 (dd, J = 5.0, 5.3, H-2″) confirm the sulfate group in the sugar moiety.

The ^{13}CNMR signals resonated at δ_C 157.3, 134.0, 178.8, 157.4 and 105.1 were characteristic of a flavonol moiety. The signals of benzene ring moiety were resonated at δ_C 115.4, 116.2, 121.5, 121.8, 145.5 and 149.1 forming an ABX system. The anomeric carbons signal observed at δ_C 106.6 and 100.5 along with further signals of the hexose moieties. Thus compound **2** was assigned as an analogue **1** (Safder et al., 2012), except slight differences in the chemical shifts of the hexose unit.

The structure of abutilin D was further confirmed by acid hydrolysis, gives quercetin and binary mixture of glycones,that identified as D -glucose and D-mannose by TLC with standard as well as by gas chromatography (GC) by comprising of retention times of their tetramethylsilane (TMS) ethers with corresponding standards. The sulphate moiety attached to D-mannose was resonated at δ_H 5.10 (dd, J = 5.0, 5.3) and was assigned to C(2″) (δ_C 82.4) through HMBC correlations (Fig. 1). The HMBC correlations showed within Table 3 allowed to assigned the structure abutilin D (**2**), as quercetin-3-O-(β-D-glucopyranosyl)-7-(2‘‘-*O*-sulfo-β-D-mannopyranoside).

Table 3 ^{1}H- ^{13}C NMR results of abutilin D **2** in C_5D_5N; δ in ppm, J in Hz.

No	Abutilin D (**2**)		
	δ_H	δ_C	HMBC
1	–	–	–
2	–	157.3	–
3	–	134.0	–
4	–	178.8	–
5	–	162.5	–
6	6.24 (d, J = 2.3)	99.6	5, 7, 10, 1″
7	–	164.1	–
8	6.45 (d, J = 2.3)	94.2	7,9,10
9	–	157.4	–
10	–	105.1	–
5-OH	13.6		
1′	–	121.8	–
2′	7.43 (d, J = 2.5)	115.4	2, 1′, 3′, 4′
3′	–	145.5	–
4′	–	149.1	–
5′	6.84 (d, J = 8.5)	116.2	1′, 3′, 4′, 6′
6′	7.70 (dd, J = 2.5, 8.5)	121.5	2, 1′, 2′, 5′
1″	4.85 (d, J = 5.0)	106.6	7, 2″, 3″
2″	5.10 (dd, J = 5.0, 5.3)	82.4	1″, 3″, 4″
3″	4.50–4.54 (m)	79.1	–
4″	4.18 (t, J = 9.0)	72.7	–
5″	3.83–3.86 (m)	79.5	–
6″	4.44–4.47 (m)	62.5	–
	4.23 (dd, J = 5.1, 5.2)		
1‴	5.32 (d, J = 7.5)	100.5	3, 2‴
2‴	4.30–4.32(m)	74.1	–
3‴	4.20–4.23 (m)	76.2	–
4‴	4.36–4.40 (m)	70.6	–
5‴	4.41–4.43 (m)	77.4	–
6‴	4.50–4.54 (m)	63.1	–
	4.27–4.29 (m)		

3.4. In-vitro antioxidant and α-glucosidase inhibition activity

The antioxidant activities of the dichloromethane extracts and pure constituents 1–2 of *A. pakistanicum* were determined by employing 1,1-diphenyl-2-picrylhydrazyl free radical (DPPH) and nitric oxide (NO) scavenging assay. The CH_2Cl_2 extracts of *A. pakistanicum* exhibited the antiradical activity against DPPH and NO with radical scavenging activities (RSA) of 92.75and 89.25% with IC_{50} values 20.35and 39.41 μg/mL respectively. In present work the CH_2Cl_2 extracts showed good abilities to quench both DPPH and NO. The ability of the *A. pakistanicum* CH_2Cl_2 extracts to quench and it was related with its observed phenol content as higher. Among pure constituents abutilins C showed significant inhibition, with IC_{50} values 41.66 (DPPH), 39.04 (NOS) μg/mL, with +ive control ascorbic acid (IC_{50}, 7.06 μg/mL) and quercetin (IC_{50}, 14.47 μg/mL) respectively, shown in Table 4.

The inhibitory activity of a-glucosidase was measured with modified method of Kim et al. It was shown that the *Abutilon pakistanicum* CH_2Cl_2 extracts exhibited excellent inhibitory activity against α-glucosidase, (extract IC_{50}: 10.85 μg/mL) as compared to standard ascarbose (IC_{50}: 5.92 μg/mL). Inhibi-

tory effects of flavonoids **1**–**2** against enzyme α-glucosidase were also investigated and abutilins C-D showed activity (Abutilin C, IC_{50} 8.27 μg/mL; Abutilin D, IC_{50}: 52.43 μg/mL) compared to +ive control as exhibited in Table 5. Optimization of assay conditions were maintained by standardizing the enzyme assay as mentioned above within experimental portion. The α-glucosidase inhobition was done by using standard protocol established after stanadadizing the assay. Phytochemical screening of the active components of *Abutilon pakistanicum* have been revealed that several types of total phenolic, flavonoids contents including, new abutilins C-D (**1**–**2**), flavonoid glycosides, are responsible for antioxidant activities as well as to inhibit the α-glucosidase activities of isolated pure constituents. These compounds were isolated and showed inhibitory effects on α-glucosidase with IC_{50} values close to that of acarbose as the standard. The results showed that compound **1** showed more potent inhibitory activity, and may be used clinically as antidiabetic agents to control blood glucose (Nguyen et al., 2019). It was observed that the *A. pakistanicum* dichloromethane extracts and and abutilins C exhibited excellent activity against antioxidant (DPPH and NO) scavenging assay and α-glucosidase inhibiton.

Table 5 Enzyme α-Glucosidase inhibition activities of dichloromethane extracts and Abutilin C-D (**1** and **2**).

Codes	Inhibition at conc. of 0.5 μg/mL (%)	IC_{50} (μg/mL)
Extract	98.81 ± 0.02	10.85 ± 0.04
Abutilin C	91.21 ± 0.07	8.27 ± 0.03
Abutilin D	81.21 ± 0.04	52.43 ± 0.05
Acarbose	**93.91 ± 0.07**	**5.92 ± 0.20**

Values are expressed as mean of five readings ± SEM.

3.5. Electronic properties and molecular descriptors

The FMOs, i.e., highest occupied molecular orbitals (HOMOs, HOMOs-1) and lowest unoccupied molecular orbitals (LUMOs, LUMOs + 1) of abutilin_C, abutilin_D and reference compounds, i.e., ascorbic acid and quercetin at level-B3LYP/TZ2P are shown in Fig. 2. In gallic acid, spatial distribution of HOMO-1 is on dihydroxyethyl, HOMO and LUMO at dihydroxyfuran-2(5H)-one while the LUMO + 1 at hydroxyl groups of furan moiety. The intra-molecular charge transfer (ICT) can be established from dihydroxyethyl (HOMO-1) to dihydroxyfuran-2(5H)-one (LUMO) and hydroxyl groups (LUMO + 1). The ICT was also observed from dihydroxyfuran-2(5H)-one (HOMO) to hydroxyl groups (LUMO + 1). In quercetin, spatial distribution of HOMO-1 can be seen on dihydroxyphenyl and benzene of the chromene, HOMO is on caqz of the chromene moiety, LUMO at the entire molecule while LUMO + 1 at the chromene unit. The ICT can established from benzene of the chromene (HOMO-1) to pyran (LUMO) and dihydroxyphenyl (HOMO-1) to chromene moiety (LUMO + 1). The ICT was found from dihydroxyphenyl (HOMO) to chromene (LUMO and LUMO + 1). In abutilin_C, spatial distribution of charge is almost similar to that of the reference compound quercetin, i.e., spatial distribution of HOMO-1 can be seen on dihydroxyphenyl and benzene of the chromene, HOMO is on dihydroxyphenyl and pyran of the chromene moiety, LUMO at the entire molecule while LUMO + 1 at the chromene unit. The ICT can be found from benzene of the chromene (HOMO-1) to pyran (LUMO) and dihydroxyphenyl (HOMO-1) to chromene moiety (LUMO + 1). The ICT was found from dihydroxyphenyl (HOMO) to chromene (LUMO and LUMO + 1). In abutilin_D, HOMO-1 is on dihydroxyphenyl ring, HOMO at dihydroxyphenyl and pyran, LUMO and LUMO + 1 at chromen unit. The ICT can be found from dihydroxyphenyl (HOMO-1 and HOMO) to chromene moiety (LUMO and LUMO + 1). The ICT can be seen from HOMO-1 → LUMO, HOMO-1 → LUMO + 1, HOMO → LUMO, HOMO → LUMO + 1 in abutilin_C, abutilin_D and reference compounds. The antioxidant ability of phytochemicals is also firmly associated with HOMO orbital spatial distribution, revealed the sites thats are most plausible within studied phytochemicals that may attacked by reactive agents and free radicals. In abutilin_C, HOMOs are overlapped on main core substantially disclosing remarkably reactive nature of the studied phytochemicals toward antioxidant and biological activity (see Fig. 3).

The energies of FMOs, i.e., HOMO-1 (E_{HOMO-1}), HOMO (E_{HOMO}), LUMO (E_{LUMO}), LUMO + 1 (E_{LUMO+1}), HOMO-LUMO energy gaps ($\Delta E_{HOMO-LUMO}$) and HOMO-1 – LUMO + 1 energy gaps ($\Delta E_{HOMO-1-LUMO+1}$) are important parameters to explore the materials electronic properties. The E_{HOMO-1}, E_{HOMO}, E_{LUMO}, E_{LUMO+1}, $\Delta E_{HOMO-LUMO}$ and $\Delta E_{HOMO-1-LUMO+1}$ of reference compounds as well as abutilin_C and abutilin_D at B3LYP/TZ2P level at S_0 in eV are exhibited within Table 2. The E_{HOMO-1} at S_0 reduce as: quercetin (-6.54) > abutilin_D (-6.68) > abutilin_C (-6.80) > ascorbic acid (-8.03). The tendency in the E_{HOMO} is as: quercetin (-5.78) > abutilin_D (-6.09) > abutilin_C (-6.34) > ascorbic acid (-6.71). The trend in the E_{LUMO} is as: ascorbic acid (-1.16) > quercetin (-1.99) > abutilin_C (-2.25) > abuti

Table 4 Antioxidant activity of dichloromethane extracts and Abutilin C-D (**1** and **2**).

Codes	DPPH assay		NO scavenging assay	
	IC_{50} ± SEM (μg/mL)	Inhibition at conc. of 0.5 μg/mL (%)	IC_{50} ± SEM (μg/mL)	Inhibition at conc. of 0.5 μg/mL (%)
Extract	20.35 ± 0.04	92.75 ± 0.93	39.41 ± 0.08	89.25 ± 0.03
Abutilin C	41.66 ± 0.08	73.37 ± 0.29	39.04 ± 0.08	68.15 ± 0.03
Abutilin D	263.20 ± 0.02	31.12 ± 0.01	275.34 ± 0.05	20.45 ± 0.67
Ascorbic Acid	**7.06 ± 1.2**	**96 ± 0.7**		
Quercetin)	–	–	**14.47 ± 0.13**	**90.21 ± 0.03**

Antioxidant assay (mean ± SEM, n = 3).

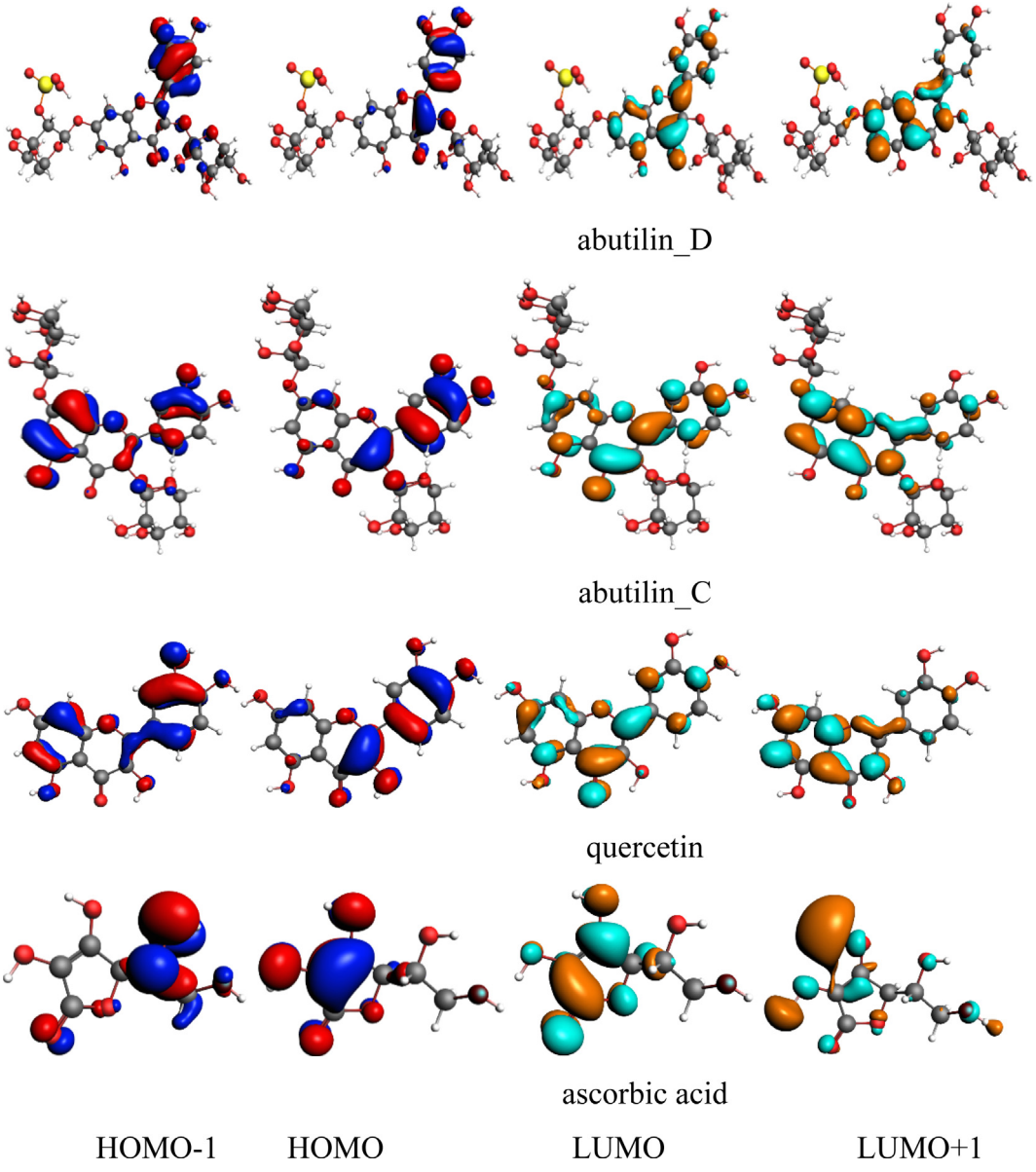

Fig. 3 Ground state charge density of FMOs of studied compounds (contour value = 0.035).

lin_D (-2.38). The tendency in the E_{LUMO+1} is as: ascorbic acid (-0.45) > quercetin (-0.91) > abutilin_C (-1.27) > abuti lin_D (-1.47). The $\Delta E_{HOMO-LUMO}$ increases in the following order: abutilin_D (3.71) < quercetin (3.79) < abutilin_C (4. 64) < ascorbic acid (5.55). The $\Delta E_{HOMO-1-LUMO+1}$ increases in the following order: abutilin_D (5.21) < abutilin_C (5.53) < quercetin (5.63) < ascorbic acid (7.58).

The work functions (W) of Au and Al are 5.10 and 4.08 eV, respectively . The hole/e injection energies (HIE/EIE) of abutilin_C, abutilin_D, and reference compounds to Au and Al electrodes are probed. For Al, (EIE = $-E_{LUMO}$ − (W of Al) has been estimated as: ascorbic acid (2.92 eV = -1.16 − (−4.08)) > quercetin (2.09 eV = -1.99 − (−4.08)) > abutilin_C (1.83 eV = -2.25 − (−4.08)) > abutilin_D (1.70 eV = -2.38 − (−4.08)). In case of Au, (EIE = $-E_{LUMO}$ − (W of Au) has been estimated as: ascorbic acid (3.94 eV = -1.16 − (−5.10)) > quercetin (3.11 eV = -1.99 − (−5.10)) > abutilin_C (2.85 eV = -2.25 − (−5.10)) > abutilin_D (2.72 eV = -2.38 − (−5.10)). The HIE were observed as: ascorbic acid (2.63 eV = − 4.08 − (-6.71) > abutilin_C (2.26 eV = − 4.08 − (-6.34) > abutilin_D (2.01 eV = − 4.08 − (-6.09) > quercetin (1.7 0 eV = − 4.08 − (-5.78) by considering Al electrode. In case of Au, HIE were observed as: gallic acid ascorbic acid (1.61 e V = − 5.10 − (-6.71) > abutilin_C (1.24 eV = − 5.10 − (-6. 34) > abutilin_D (0.99 eV = − 5.10 − (-6.09) > quercetin (0. 68 eV = − 5.10 − (-5.78). It was recognized that for better e/hole injection ability, Al/Au would be more suitable electrode.

Global chemical reactivity descriptors (GCRD) are important parameters to realize the reactivity and structure stability. Here, we estimated various GCRD parameters like chemical hardness-η, chemical potential-μ, electronegativity-χ, softness-S and electrophilicity index-ω of isoflavones using HOMO and LUMO energy values, see Table 6 (computational

details can be found in SI). The η value of phytochemical is aromaticity interrelated (Geerlings et al., 2003; Vektariene et al., 2009). The μ value express its electron tendency to rush out with its electronic cloud. The η value also symbolizes electronic cloud obstruction extent deformation and ω signifies the stabilization energy when the systenm is saturated by es from the external environment.

The Molecular electrostatic potential (MEP) maps are important to envision the charged region of phytochemicals. In Fig. 4, the MEP mapped for pure constituents and reference compounds are displayed in color visual images. The red, blue shades within figure identifies the sophisticated -ive and +ive potential regions which would be favorable for electrophilic/nucleophilic attack, respectively. The concentrated negative electrostatic potential can be seen on the oxygen atoms of –OH while +ive potential is determined on hydrogen atoms of –OH.

The Hirshfeld charges of the abutilin_C, abutilin_D and reference compounds are demonstrated within Fig. S1. The -ive charge can be located on the -O atoms while +ive charge on -H atoms. These results showed that studied compounds have favorable sites for electrophilic/nucleophilic attacks would bring about greater antioxidant potential.

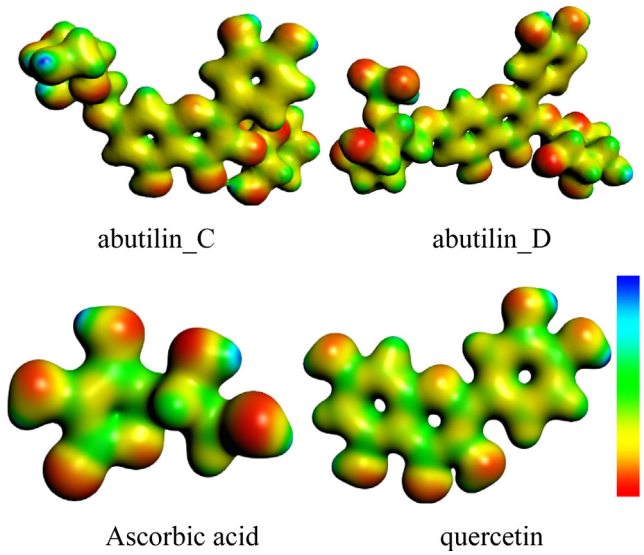

Fig. 4 Molecular electrostatic potential surfaces views of studied compounds.

3.6. Molecular docking

As far as we know, no theoretical studies for Abtulin_C and Abtulin_D compounds were conducted especially resistance with NADPH (PDB ID-2CDU) enzyme. We investigated the interactions of the studied phytochemicals with NADPH crystal structure in order to attain better understanding on the potency and SAR studies. Molecular docking was employed by inserting isolated phytochemicals (Abtulin_C and Abtulin_D) into the binding site of NADPH crystal structure. The determination of the 2CDU NADPH enzyme structure exceuted with Worldwide Protein Data Bank. The 2CDU NADPH enzyme crystal structure without H_2O and inhibitors are displayed within Fig. 5. The binding energies values between phytochemicals and 2CDU NADPH enzyme (active sites in the phytochemicals and enzyme) are displayed within Table 7 and Fig. 6. The hydrogen bonding between keto oxygen of Abtulin_C and hydrogen of ARG308 was observed with the distance 1.7 Angstrom. Another hydrogen bonding was found between hydrogen atom of Abtulin_C and oxygen of GLN18 was observed with the distance 1.8 Angstrom. The hydrogen bonding between hydrogen of Abtulin_D and keto oxygen of GLY254 was observed with the distance 2.3 and 2.9 Angstrom. Another hydrogen bonding was found between hydrogen atom of Abtulin_D and oxygen of LYS255 was observed with the distance 2.2 Angstrom. One more hydrogen bonding was found between oxygen atom of Abtulin_D and hydrogen of SER273 was observed with the distance 2.8 Angstrom. The +ive binding energy of Abtulin_D mean that affin-

Table 6 The ground state ground state HOMO energies (E_{HOMO} *and* E_{HOMO-1}), LUMO energies (E_{LUMO} *and* E_{LUMO+1}), energy gaps, IP, EA, η, μ, S, χ and ω in eV of abutilin_C, abutilin_D and reference compounds.

Parameters	Ascorbic Acid	quercetin	abutilin_C	abutilin_D
E_{HOMO}	−6.71	−5.78	−6.34	−6.09
E_{HOMO-1}	−8.03	−6.54	−6.80	−6.68
E_{LUMO}	−1.16	−1.99	−2.25	−2.38
E_{LUMO+1}	−0.45	−0.91	−1.27	−1.47
$\Delta E_{HOMO-LUMO}$	5.55	3.79	4.64	3.71
$\Delta E_{HOMO-1-LUMO+1}$	7.58	5.63	5.53	5.21
Hardness (η)	2.54	1.81	2.53	2.12
Potential (μ)	−4.17	−3.97	−3.80	−3.97
Softness (S)	1.31	1.60	1.25	1.44
Electronegativity (χ)	4.17	3.97	3.81	3.97
Electrophilic index (ω)	3.42	4.35	2.85	3.72
Ionization potential (IP)	6.71	5.78	6.34	6.09
Electron affinity (EA)	1.16	1.99	2.25	2.38

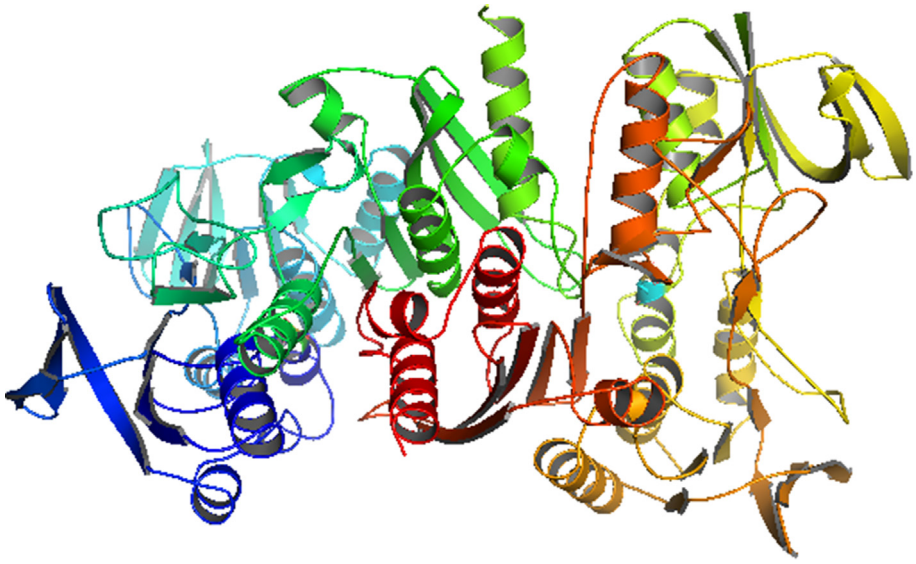

Fig. 5 Crystal structure of the NADPH (PDB ID-2CDU) enzymes (water molecules and inhibitors are removed for clarity).

Table 7 Docking simulation results with binding Energy (BE), sequence between the referenced and isolated compounds with NADPH (PDB ID-2CDU) enzyme.

Compounds	BE	Binding sequence
Abtulin_C	−1.05	GLN18, ARG308, LYS318
Abtulin_D	1.91	GLY254, LYS255, SER273

ity is too low. As a results of association of phytochemicals with a target drug binding energy is released, which leads to its overall energy reduction. This binding energy decompress also counterbalance mpensates for any phytochemical transformation therefrom energy minimal to its confined conformation along with the relevant protein. As a consequences of phytochemical binding with protein more energy released resulted enhanced tendency of association of phytochemical

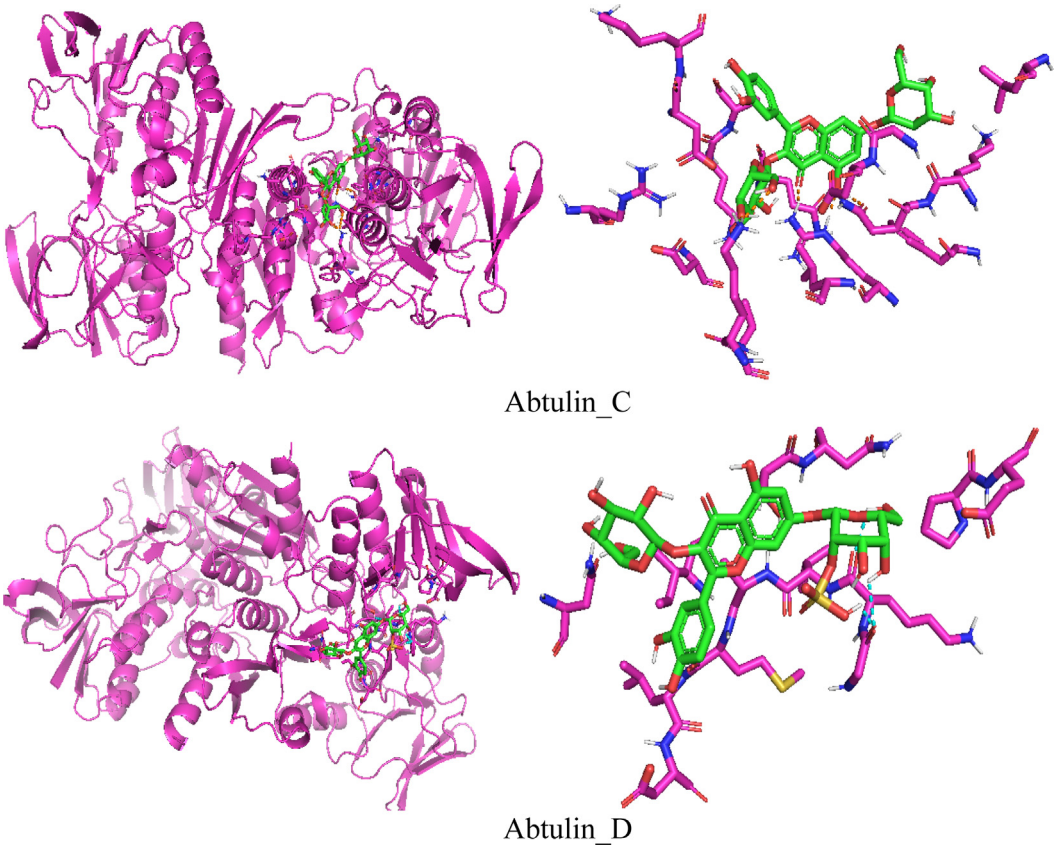

Fig. 6 Docking simulation of the interaction between isolated compounds and NADPH enzyme.

among with relevant protein. Based on reduction within binding energy made more consistent complex, *i.e*., phytochemicals having −1.05 Kcal/mol binding energy, is more stable than ligand having 1.91 Kcal/mol binding energy. The vale of Gibbs Free Energy –ive is preferable for its better binding. The obtained docking results for Abtulin_C were found better that is illuminating that this compound would be better antioxidant than the Abtulin_D which is in good agreement with our experimental studies.

4. Conclusions

The bioguided fractionations of crude methanolic extract of *A. pakistanicum* revealed the higher concentrations of phenolic and flavonoids within dichloromethane soluble fractions indicating the biological active constituents. Further bioguided isolation of dichloromethane soluble portions affoarded new abutilins C-D (**1**–**2)** of flavonoids class**.** Their structures were determined by advanced spectroscopic methods including FAB-MS, ESI-MS, 1D and 2D-NMR experiments. In order to determine active antioxidant ingredients from this portions,), two new flavonoid glycosides, were isolated and characterized from the dichloromethane extract of the whole plant of *Abutilon pakistanicum*. The structures of these compounds were elucidated by spectroscopic data including FAB-MS, ESI-MS, 1D and 2D-NMR experiments. The dichloromethane and pure compounds abutilins C-D (**1**–**2)** were evaluated for antioxidant (DPPH and No scavenging) and α-glucosidase inhibitory assay. The abutilins C showed significant antioxidant (NOS) and α-glucosidase activity with IC_{50} values 39.04 and 8.27 μg/mL respectively and act as dual inhibitors. The ICT was found from highest occuppied to lowest unoccupied molecular orbitals. The Hirshfeld charges, molecular electrostatic potentials and molecular docking studies showed that abutilin_C would be better biological active compound than its counterpart.

Declaration of Competing Interest

The authors declare that they have no known competing financial interests or personal relationships that could have appeared to influence the work reported in this paper.

Acknowledgement

The authors express their gratitude to ICCBS, H. E. J. Research Institute of Chemistry, University of Karachi, Karachi, Pakistan, on providing research facilities for this work. We extend appreciation to the Deanship of Scientific Research at King Khalid University for funding this work through research groups program under grant number R.G.P.2/76/41.

References

Ali, B., Ibrahim, M., Hussain, I., Hussain, N., Imran, M., Nawaz, H., Jan, S., Khalid, M., Ghous, T., Akash, M.S.H., 2014. Pakistamide c, a new sphingolipid from abutilon pakistanicum. Revista Brasileira de Farmacognosia 24 (3), 277–281.

Ali, B., Imran, M., Hussain, R., Ahmed, Z., Malik, A., 2010. Structural determination of abutilins a and b, new flavonoids from abutilon pakistanicum, by 1d and 2d nmr spectroscopy. Magn. Reson. Chem. 48 (2), 159–163.

Ali, B., Mehmood, R., Mughal, U.R., Malik, A., Safder, M., Hussain, R., Imran, M., Tareen, R.B., 2012. Eremosides a–c, new iridoid glucosides from eremostachys loasifolia. Helv. Chim. Acta 95 (4), 586–593.

Anastassova, N.O., Mavrova, A.T., Yancheva, D.Y., Kondeva-Burdina, M.S., Tzankova, V.I., Stoyanov, S.S., Shivachev, B.L., Nikolova, R.P., 2018. Hepatotoxicity and antioxidant activity of some new n, n′-disubstituted benzimidazole-2-thiones, radical scavenging mechanism and structure-activity relationship. Arab. J. Chem. 11 (3), 353–369. https://doi.org/10.1016/j.arabjc.2016.12.003.

Cenobio-Galindo, A.d.J., Ocampo-López, J., Reyes-Munguía, A., Carrillo-Inungaray, M.L., Cawood, M., Medina-Pérez, G., Fernández-Luqueño, F., Campos-Montiel, R.G., 2019. Influence of bioactive compounds incorporated in a nanoemulsion as coating on avocado fruits (persea americana) during postharvest storage: Antioxidant activity, physicochemical changes and structural evaluation. Antioxidants 8 (10), 500. https://doi.org/10.3390/antiox8100500.

Geerlings, P., De Proft, F., Langenaeker, W., 2003. Conceptual density functional theory. Chem. Rev. 103 (5), 1793–1874.

Genovese, C., Acquaviva, R., Ronsisvalle, S., Tempera, G., Antonio Malfa, G., D'Angeli, F., Ragusa, S., Nicolosi, D., 2020. In vitro evaluation of biological activities of orobanche crenata forssk. Leaves extract. Natural Prod. Res. 34 (22), 3234–3238. https://doi.org/10.1080/14786419.2018.1552697.

Halabalaki, M., Urbain, A.l., Paschali, A., Mitakou, S., Tillequin, F. O., Skaltsounis, A.-L. 2011. Quercetin and kaempferol 3-o-[α-l-rhamnopyranosyl-(1→ 2)-α-l-arabinopyranoside]-7-o-α-l-rhamnopyranosides from anthyllis hermanniae: Structure determination and conformational studies. J. Nat. Prod. 74(9), 1939–1945.

Irfan, A., 2019. Comparison of mono- and di-substituted triphenylamine and carbazole based sensitizers @(tio2)38 cluster for dye-sensitized solar cells applications. Comp. Theor. Chem. 1159, 1–6. https://doi.org/10.1016/j.comptc.2019.04.008.

Irfan, A., Al-Sehemi, A.G., Assiri, M.A., Mumtaz, M.W., 2019a. Exploring the electronic, optical and charge transfer properties of acene-based organic semiconductor materials. Bull. Mater. Sci. 42 (4), 145. https://doi.org/10.1007/s12034-019-1838-9.

Irfan, A., Assiri, M., Al-Sehemi, A.G., 2018. Exploring the optoelectronic and charge transfer performance of diaza[5]helicenes at molecular and bulk level. Org. Electron. 57, 211–220. https://doi.org/10.1016/j.orgel.2018.03.022.

Irfan, Ahmad, Chaudhry, Aijaz Rasool, Al-Sehemi, Abdullah G., Assiri, Mohammed A., Hussain, Arshad, 2019b. Charge carrier and optoelectronic properties of phenylimidazo[1,5-a]pyridine-containing small molecules at molecular and solid-state bulk scales. Comp. Mater. Sci. 170, 109179. https://doi.org/10.1016/j.commatsci.2019.109179.

Irfan, A., Imran, M., Al-Sehemi, A.G., Assiri, M.A., Hussain, A., Khalid, N., Ullah, S., Abbas, G., 2020a. Quantum chemical, experimental exploration of biological activity and inhibitory potential of new cytotoxic kochiosides from kochia prostrata (l.) schrad. J. Theor. Comput. Chem. 19 (05), 2050012. https://doi.org/10.1142/s0219633620500121.

Irfan, A., Imran, M., Thomas, R., Mumtaz, M.W., Basra, M.A.R., Ullah, S., Al-Sehemi, A.G., Assiri, M.A., 2020b. Hole transport nature exploration of 4,4-difluoro-8-(c4h3x)-4-bora-3a,4a-diaza-s-indacene (x = o, s, se) (bodipy) systems. Mol. Simul. 46 (17), 1334–1339. https://doi.org/10.1080/08927022.2020.1820005.

Irfan, Ahmad, Imran, Muhammad, Thomas, Renjith, Mumtaz, Muhammad Waseem, Qayyum, Muhammad Abdul, Ullah, Sami, Assiri, Mohammed A., Al-Sehemi, Abdullah G., 2020c. Exploration of electronic nature and intrinsic mobility of 10-(1,3-dithiol-2-ylidene)anthracene based organic semiconductor materials. Optik 224, 165530. https://doi.org/10.1016/j.ijleo.2020.165530.

Irfan, A., Jin, R., Al-Sehemi, A.G., Asiri, A.M., 2013. Quantum chemical study of the donor-bridge-acceptor triphenylamine based sensitizers. Spectrochimica Acta A 110, 60–66. https://doi.org/10.1016/j.saa.2013.02.045.

Irfan, A., Mahmood, A., Al-Sehemi, A.G., Ahmad, F., 2019c. Experimental and theoretical study of planar small molecule acceptor for organic solar cells. J. Mol. Struct. 1196, 169–175. https://doi.org/10.1016/j.molstruc.2019.06.035.

Meng, J.-M., Cao, S.-Y., Wei, X.-L., Gan, R.-Y., Wang, Y.-F., Cai, S.-X., Xu, X.-Y., Zhang, P.-Z., Li, H.-B., 2019. Effects and mechanisms of tea for the prevention and management of diabetes mellitus and diabetic complications: An updated review. Antioxidants 8 (6), 170.

Miyazawa, Mitsuo, Hisama, Masayoshi, 2003. Antimutagenic activity of flavonoids from chrysanthemum morifolium. Biosci. Biotechnol. Biochem. 67 (10), 2091–2099.

Nasri, H., Shirzad, H., Baradaran, A., Rafieian-Kopaei, M., 2015. Antioxidant plants and diabetes mellitus. J. Res. Med. Sci. Off. J. Isfahan Univ. Med. Sci. 20 (5), 491. https://doi.org/10.4103/1735-1995.163977.

Nguyen, Hai Xuan, Nguyen, Loc Thanh, Van Do, Truong Nhat, Le, Tho Huu, Dang, Phu Hoang, Tran, Hung Manh, Nguyen, Nhan Trung, Nguyen, Mai Thanh Thi, 2019. A new phenolic acid from the wood of mangifera gedebe. Nat. Prod. Res., 1–4 https://doi.org/10.1080/14786419.2019.1680666.

Preat, J., Jacquemin, D., Perpète, E.A., 2010. Design of new triphenylamine-sensitized solar cells: A theoretical approach. Environ. Sci. Technol. 44 (14), 5666–5671. https://doi.org/10.1021/es100920j.

Preat, J., Michaux, C., Jacquemin, D., Perpète, E.A., 2009. Enhanced efficiency of organic dye-sensitized solar cells: Triphenylamine derivatives. J. Phys. Chem. C 113 (38), 16821–16833. https://doi.org/10.1021/jp904946a.

Rammohan, Aluru, Bhaskar, Baki Vijaya, Camilo, Alexandre, Gunasekar, Duvvuru, Gu, Wei, Zyryanov, Grigory V., 2020. In silico, in vitro antioxidant and density functional theory based structure activity relationship studies of plant polyphenolics as prominent natural antioxidants. Arabian J. Chem. 13 (2), 3690–3701. https://doi.org/10.1016/j.arabjc.2019.12.017.

Sadeer, N.B., Rocchetti, G., Senizza, B., Montesano, D., Zengin, G., Uysal, A., Jeewon, R., Lucini, L., Mahomoodally, M.F., 2019. Untargeted metabolomic profiling, multivariate analysis and biological evaluation of the true mangrove (rhizophora mucronata lam.). Antioxidants 8 (10), 489.

Safder, Muhammad, Mehmood, Rashad, Ali, Bakhat, Mughal, Uzma Rasheed, Malik, Abdul, Jabbar, Abdul, 2012. New secondary metabolites from asphodelus tenuifolius. Helv. Chim. Acta 95 (1), 144–151.

Saffarzadeh-Matin, Shohreh, Khosrowshahi, Fatemeh Masoudi, 2017. Phenolic compounds extraction from iranian pomegranate (punica granatum) industrial waste applicable to pilot plant scale. Ind. Crops Prod. 108, 583–597.

Sharma, Ajay, Cannoo, Damanjit Singh, 2017. A comparative study of effects of extraction solvents/techniques on percentage yield, polyhenolic composition, and antioxidant potential of various extracts obtained from stems of n epeta leucophylla: Rp-hplc-dad assessment of its polyhenolic constituents. J. Food Biochem. 41 (2), e12337. https://doi.org/10.1111/jfbc.2017.41.issue-210.1111/jfbc.12337.

Tanase, C., Mocan, A., Coşarcă, S., Gavan, A., Nicolescu, A., Gheldiu, A.-M., Vodnar, D.C., Muntean, D.-L., Crişan, O., 2019. Biological and chemical insights of beech (fagus sylvatica l.) bark: A source of bioactive compounds with functional properties. Antioxidants 8 (9), 417.

Valko, Marian, Jomova, Klaudia, Rhodes, Christopher J., Kuča, Kamil, Musílek, Kamil, 2016. Redox-and non-redox-metal-induced formation of free radicals and their role in human disease. Arch. Toxicol. 90 (1), 1–37.

Vats, Sharad, 2016. Effect of initial temperature treatment on phytochemicals and antioxidant activity of azadirachta indica a. Juss. Appl. Biochem. Biotechnol. 178 (3), 504–512.

Vektariene, A., Vektaris, G., Svoboda, J., 2009. A theoretical approach to the nucleophilic behavior of benzofused thieno [3, 2-b] furans using dft and hf based reactivity descriptors. Arkivoc 7, 311–329.

Wazzan, Nuha, Irfan, Ahmad, 2019. Exploring the optoelectronic and charge transport properties of pechmann dyes as efficient oled materials. Optik 197, 163200. https://doi.org/10.1016/j.ijleo.2019.163200.

Zhu, Jianzhong, Zhang, Bin, Wang, Bingxu, Li, Chao, Fu, Xiong, Huang, Qiang, 2019. In-vitro inhibitory effects of flavonoids in rosa roxburghii and r. Sterilis fruits on α-glucosidase: Effect of stomach digestion on flavonoids alone and in combination with acarbose. J. Funct. Foods 54, 13–21.